A SMOOTH TRANSITION MODEL BETWEEN KINETIC AND DIFFUSION EQUATIONS*

PIERRE DEGOND† AND SHI JIN‡

Abstract. This paper presents a model which provides a smooth transition between a kinetic and a diffusion domain. The idea is to use a buffer zone, in which both diffusion and kinetic equations will be solved. The solution of the original kinetic equation will be recovered as the **sum** of the solutions of these two equations. We use an artificial connecting function which makes the equation on each domain degenerate at the end of the buffer zone. Thus no boundary condition is needed at the transition point. This model avoids the delicate issue of finding the interface condition or iteration in a typical domain decomposition method that couples a kinetic equation with hydrodynamic equations. A new asymptotic preserving method for this model is introduced, and numerical examples are used to validate this new model and the new numerical method.

Key words. Kinetic-fluid coupling, Transport equation, Diffusion approximation, Asymptotic preserving schemes

AMS subject classifications. 82B40, 82B80, 82C40, 82C70, 82C80, 76R50

1. Introduction.

The collision transition rate in a kinetic transport process is often position-dependent, varies from order unity in certain parts of the domain to an order of magnitude much smaller in other parts of the domain. For instance, in radiative transfer, the transition from a transparent to an opaque medium involves a change of collision rate by several orders of magnitude. Similarly, in stellar astrophysics, the magnitude of the photon transition rate can change by decades from the core of a star to its surface. When the collision rate is large, the diffusion equation is valid and much more efficient to solve numerically. In the domain where the collision rate is small, solving the more expensive kinetic transport equation in the phase space is necessary. Although one can solve the transport equation in the entire domain, to reduce the computational cost, it is more advocated to use a domain decomposition method that couples the diffusion equation with the transport equation.

Domain decomposition methods matching kinetic and hydrodynamic or diffusion models have received a lot of attention in the past 15 years. Some of the methods have been proposed in [3], [7], [14], [15], [18], [19], [25], [26], [28], [29], [33], [34], [37]. Typically a domain decomposition is done by an iteration procedure at each time step in which the diffusion and the transport equation are solved alternately until convergence of the successive approximation is reached, or through an interface condition which provides the boundary conditions for each subdomain [18].

Other strategies are hybrid strategies, in which two equations are solved simultaneously: a fluid equation for the equilibrium part of the distribution function and a kinetic equation for perturbation to the equilibrium part. Recently, hybrid methods have been derived by a domain decomposition method *in velocity space* [11], [12], [13]. These methods bear similarities with the δf method developed by the plasma physicists [8].

In this paper we present a new approach to the domain decomposition method using a buffer zone, in which both diffusion and kinetic equations will be solved.

*Supports by the European network HYKE, funded by the EC as contract HPRN-CT-2002-00282, and by NSF grant DMS0196106, are gratefully acknowledged.

†MIP, UMR 5640 (CNRS-UPS-INSA), Université Paul Sabatier, 118, route de Narbonne, 31062 TOULOUSE cedex, FRANCE (degond@mip.ups-tlse.fr).

‡Department of Mathematics, University of Wisconsin, Madison, WI 53706 (jin@math.wisc.edu).

The solution of the original transport equation will be recovered as the *sum* of the solutions of these two equations. In this way, our strategy departs from strategies based on domain decomposition with overlap, in which *each* of the models represents the *full* solution. Unlike a typical domain decomposition where an interface condition has to be worked out in order to provide the boundary condition for each decomposed domain [18], we use an artificial connecting function which makes the equation on each domain degenerate at the end of the buffer zone, thus no boundary condition is needed at the transition point. Thus the delicate issue of finding the interface condition is completely avoided, nor will this method requires any iteration at any given time step to match the solution of the two subdomains.

The paper is organized as follows. In the next section, we introduce the coupling technique and carry out some elementary analysis on its properties. A new asymptotic-preserving numerical scheme for this coupling model is derived in Section 3. We present numerical experiments in Section 4 to validate this new model and the numerical method introduced, and conclude in Section 5.

2. The coupling methodology.

2.1. The transport equation and its diffusion limit. We present the method on a simple kinetic equation, the one-group transport equation in slab geometry [10]. Let $f(x,\mu,t)$ represent the particle phase-space density, where $x \in \mathbb{R}$ is the (one-dimensional) position variable, $\mu \in [-1,1]$ is the cosine of the angle between the velocity and the x-axis, and t is the time. In this model, the magnitude of the particle velocities are equal and normalized to 1. Then, the transport equation is

$$\partial_t f + \mu \partial_x f = Q(f)\,, \tag{2.1}$$

$$Q(f) = \int_{-1}^{1} S(x,\mu,\mu')(f(x,\mu',t) - f(x,\mu,t))\,d\mu'\,. \tag{2.2}$$

The left hand-side of (2.1) describes the motion of the particles along the x axis with velocity μ while the operator Q takes into account the particle interactions with the medium. $S(x,\mu,\mu')$ is the collision transition rate from μ to μ' at point x. In the formulation (2.2), we implicitly assumed that these interactions preserve particle number, i.e.

$$\int_{-1}^{1} Q(f)\,d\mu = 0\,. \tag{2.3}$$

This will be sufficient for our purpose. In practical cases, like neutron transport or radiative transfer, it is necessary to include non-conservative cases (like neutron multiplication or photon absorption/emission) but these effects are not essential and can be easily incorporated into our formulation. Eq. (2.1) must be supplemented with an initial condition $f_0(x,\mu)$ and suitable boundary conditions. A particular case is when S does not depend on μ and μ': $S(x,\mu,\mu') = \sigma(x)/2$ where σ is the collision frequency. Then:

$$Q(f) = \sigma(x)\left[\frac{1}{2}\int_{-1}^{1} f(x,\mu',t)\,d\mu' - f(x,\mu,t)\right]\,, \tag{2.4}$$

is (up to a multiplicative factor) a projection operator onto the functions independent of μ.

When the particle interactions with the medium are very frequent, i.e. when Q is 'large', the numerical resolution of (2.1) becomes extremely time consuming, and it is worth using the asymptotic model obtained when Q 'tends to infinity'. We introduces a new set of 'macroscopic variables' x' and t' according to

$$x' = \varepsilon x\,, \quad t' = \varepsilon^2 t\,,$$

where ε denotes the ratio of the microscopic to the macroscopic scale. Typically, ε is the ratio of the particle mean-free path (related to a typical value of S) to the size of the problem under consideration, and is called the Knudsen number. After using this change of variables and dropping the primes for simplicity, one gets

$$\varepsilon^2 \partial_t f^\varepsilon + \varepsilon \mu \partial_x f^\varepsilon = Q(f^\varepsilon)\,, \tag{2.5}$$

In the limit $\varepsilon \to 0$, f^ε converges towards the solution of a diffusion equation. More precisely, we have (see e.g. [5]):

Lemma 2.1. *$f^\varepsilon \to n(x,t)$ where n is a solution of*

$$\partial_t n - \partial_x (D(x) \partial_x n) = 0\,, \tag{2.6}$$

with initial condition $n|_{t=0} = \frac{1}{2}\int f_0(x,\mu)\,d\mu$. The diffusion constant D is related to Q by:

$$D(x) = -\frac{1}{2}\int_{-1}^{1} Q^{-1}(\mu)\,\mu\,d\mu > 0\,. \tag{2.7}$$

We shall not be more precise on the functional spaces and refer to [5, 17] for details. The definition of Q^{-1} needs a few words of explanation. Indeed Q has the following properties as an operator acting on functions of μ (see e.g. [5]):

Lemma 2.2. *Suppose that $0 < C_0 \le S \le C_1 < \infty$. Then Q is a bounded self-adjoint non-positive operator on $L^2(-1,1)$. Furthermore:*
(i) $\mathrm{Ker\,Q}$ *consists of constant functions with respect to μ.*
(ii) $\mathrm{Im\,Q} = (\mathrm{Ker\,Q})^\perp = \{\mathrm{g}\ \textit{s.t.}\ \int \mathrm{g}\,\mathrm{d}\mu = 0\}$.
(iii) Q is invertible from $(\mathrm{Ker\,Q})^\perp$ *to* $(\mathrm{Ker\,Q})^\perp$*. Its (pseudo)-inverse is denoted by Q^{-1}.*

It is worth summarizing the main steps of the proof.

Proof of Lemma 2.1: We use the Hilbert expansion:

$$f^\varepsilon = f^{(0)} + \varepsilon f^{(1)} + \varepsilon^2 f^{(2)} + O(\varepsilon^3)\,. \tag{2.8}$$

We insert this expansion into (2.5) and identify terms of equal powers of ε. This leads to the sequence of equations:

$$Q(f^{(0)}) = 0\,, \tag{2.9}$$
$$Q(f^{(1)}) = \mu \partial_x f^{(0)}\,, \tag{2.10}$$
$$Q(f^{(2)})) = \mu \partial_x f^{(1)} + \partial_t f^{(0)}\,. \tag{2.11}$$

With (2.9) and Lemma 2.2 (i), we deduce that $f^{(0)}$ does not depend on μ. We denote by $n(x,t) = f^{(0)}(x,\mu,t)$.

Eq. (2.10) simplifies into

$$Q(f^{(1)}) = \mu \partial_x n\,. \tag{2.12}$$

Its right-hand side is an odd function of μ and therefore, integrated against any constant function, yields 0. Therefore, it belongs to $(\operatorname{Ker} Q)^{\perp}$. By Lemma 2.2 (iii), we can invert (2.12) in $(\operatorname{Ker} Q)^{\perp}$ and get

$$f^{(1)} = Q^{-1}(\mu)\partial_x n\,. \tag{2.13}$$

For the most general solution of (2.12), we should add an element of $(\operatorname{Ker} Q)$, i.e. a function of (x,t) only. However, we can discard it because it has no influence on the result. This point is left to the reader.

Eq. (2.11) is solvable for $f^{(2)}$ if and only if its right-hand side is orthogonal to the functions independent of μ. Therefore, the solvability condition of (2.11) reads:

$$\partial_t n + \partial_x j = 0\,, \tag{2.14}$$

with

$$j = \frac{1}{2}\int_{-1}^{1} f^{(1)}\mu\, d\mu\,. \tag{2.15}$$

Inserting (2.13) into (2.15), we get that $j = -D\partial_x n$ with D given by (2.7). Finally, with (2.14), we get (2.6). The fact that D is positive comes from the positive definiteness of $-Q$ on $(\operatorname{Ker} Q)^{\perp}$. ∎

Note that in the case (2.4), $D = 1/(3\sigma)$.

The proof of Lemma 2.1 relies on the fact that S (or σ) is everywhere of order unity (with respect to ε). However, S is position-dependent and there are numerous situations in which it is of order unity in certain parts of the domain while it is much smaller (of order ε or ε^2) in other parts of the domain. The diffusion equation is only valid when S is of order unity. If S is smaller, solving the transport equation is necessary. Therefore, one needs to couple the diffusion equation in the regions where S is of order unity, to the transport equation in the regions where it is smaller.

2.2. The coupling method. This problem has been adressed by many authors and methods (see the bibliography in the introduction). Our approach is novel and consists in introducing a buffer zone in which both diffusion and kinetic equations will be solved. The solution of the initial transport equation will be recovered as the *sum* of the solutions of these two equations. In this way, our strategy departs from strategies based on domain decomposition with overlap, in which *each* of the models represents the *full* solution.

The buffer interval is denoted by $[a,b]$. We introduce a smooth function $h(x)$ such that

$$\begin{cases} h(x) = 1, & \text{for} \quad x \le a\,, \\ h(x) = 0, & \text{for} \quad x \ge b\,, \\ h(x) \in (0,1), & \text{for} \quad a \le x \le b\,. \end{cases}$$

We consider the following coupled system for two distribution functions f_L and f_R:

$$\varepsilon^2\partial_t f_L^\varepsilon + \varepsilon h\mu\partial_x f_L^\varepsilon + \varepsilon h\mu\partial_x f_R^\varepsilon = h(Q(f_L^\varepsilon) + Q(f_R^\varepsilon))\,, \tag{2.16}$$

$$\varepsilon^2\partial_t f_R^\varepsilon + \varepsilon(1-h)\mu\partial_x f_L^\varepsilon + \varepsilon(1-h)\mu\partial_x f_R^\varepsilon = (1-h)(Q(f_L^\varepsilon) + Q(f_R^\varepsilon))\,, \tag{2.17}$$

with initial data

$$f_L^\varepsilon|_{t=0} = hf_0\,, \quad f_R^\varepsilon|_{t=0} = (1-h)f_0\,. \tag{2.18}$$

We first note the following:

LEMMA 2.3. *If f_L^ε and f_R^ε are the solution of problem (2.16), (2.17) with initial data (2.18), then $f = f_L^\varepsilon + f_R^\varepsilon$ is the solution of problem (2.5) with initial condition f_0.*

Proof: Just add up eqs. (2.16) and (2.17). ∎

We note that in reality, (2.16) is posed on the interval $(-\infty, b)$ and (2.17) on $(a, +\infty)$ since h vanishes for $x > b$ and $1-h$ for $x < a$. Additionally, since h (respectively $1-h$) is in factor of the space derivative operator does in (2.16) (resp. (2.17)), *no boundary condition is required for f_L^ε at $x = b$ (resp. for f_R^ε at $x = a$).*

Now, we assume that S is of order ε^2 in the interval $(-\infty, a)$, while it is of order 1 in $(a, +\infty)$. Therefore, we shall only be allowed to perform the diffusion approximation on f_R^ε while f_L^ε will have to stay untouched. For this purpose, we rewrite (2.17) according to

$$\begin{aligned}&\varepsilon^2 \partial_t f_R^\varepsilon + \varepsilon(1-h)\mu\partial_x f_R^\varepsilon - (1-h)Q(f_R^\varepsilon) \\ &= -\varepsilon(1-h)\mu\partial_x f_L^\varepsilon + (1-h)Q(f_L^\varepsilon)\,,\end{aligned} \tag{2.19}$$

and we consider that the terms at the right-hand side are of order ε^2. The following proposition states what the diffusion approximation $\varepsilon \to 0$ of this equation is.

PROPOSITION 2.4. *Consider eq. (2.19) where the right-hand side is treated as an $O(\varepsilon^2)$ term. Then as $\varepsilon \to 0$, $f_R^\varepsilon \sim n_R^\varepsilon$ where $n_R^\varepsilon = n_R^\varepsilon(x,t)$ is a solution of the following diffusion equation:*

$$\partial_t n_R^\varepsilon - (1-h)\partial_x[D(x)\partial_x n_R^\varepsilon] + (1-h)\partial_x j_L^\varepsilon = 0\,, \tag{2.20}$$

where D is given by (2.7) and

$$j_L^\varepsilon = \frac{1}{2\varepsilon}\int_{-1}^{1} f_L^\varepsilon \mu \, d\mu\,. \tag{2.21}$$

Since ε tends to 0 only in some terms and not in others, we cannot speak of convergence but rather, of asymptotic equivalence, hence the use of the symbol $\sim$. Again, (2.20) is a diffusion equation on the interval $[a, +\infty)$. However, since $1-h$ vanishes at $x = a$, *the diffusion operator is degenerate at this point and no boundary condition is required.*

Proof: We again write the Hilbert expansion $f_R^\varepsilon = f_R^{(0)} + \varepsilon f_R^{(1)} + \varepsilon^2 f_R^{(2)} + O(\varepsilon^3)$. The computations of $f_R^{(0)} = n_R$ and of $f_R^{(1)}$ are the same as in Lemma 2.1. Indeed, the right-hand side of (2.19) being of order ε^2 does not have any contribution to (2.9) and (2.10). The only change is in (2.11), which becomes:

$$\begin{aligned}(1-h)Q(f_R^{(2)}) &= (1-h)\mu\partial_x f_R^{(1)} + \partial_t f_R^{(0)} \\ &\quad + \frac{1}{\varepsilon}(1-h)\mu\partial_x f_L^\varepsilon - \frac{1}{\varepsilon^2}(1-h)Q(f_L^\varepsilon)\,.\end{aligned} \tag{2.22}$$

We note that the last two terms are of order 1 by our hypothesis, despite their apparent dependence on ε. Integrating (2.22) with respect to μ in order to express the solvability condition for f_R^2, we obtain:

$$\partial_t n_R^\varepsilon + (1-h)\partial_x j_R^\varepsilon = -(1-h)\partial_x\Big(\frac{1}{2\varepsilon}\int_{-1}^{1} f_L^\varepsilon \mu\, d\mu\Big)\,,$$

because the contribution of $Q(f_L^\varepsilon)$ vanishes after integration with respect to μ, by (2.3). This leads to (2.20) and concludes the proof. ∎

The coupled kinetic-diffusion model is now written as follows:

$$\varepsilon^2\partial_t f_L^\varepsilon + \varepsilon h\mu\partial_x f_L^\varepsilon + \varepsilon h\mu\partial_x f_R^\varepsilon = h(Q(f_L^\varepsilon)+Q(f_R^\varepsilon)), \qquad -\infty < x \le b \quad (2.23)$$
$$\partial_t n_R^\varepsilon - (1-h)\partial_x(D(x)\partial_x n_R^\varepsilon) + (1-h)\partial_x j_L^\varepsilon = 0, \quad a \le x < \infty \quad (2.24)$$
$$f_R^\varepsilon = n_R^\varepsilon + \varepsilon Q^{-1}(\mu)\partial_x n_R^\varepsilon, \quad (2.25)$$
$$j_L^\varepsilon = \frac{1}{2\varepsilon}\int_{-1}^{1} f_L^\varepsilon \mu\, d\mu, \quad (2.26)$$

with initial data

$$f_L^\varepsilon|_{t=0} = hf_0, \quad f_R^\varepsilon|_{t=0} = (1-h)f_0, \quad n_R^\varepsilon|_{t=0} = \frac{1}{2}(1-h)\int_{-1}^{1} f_0\, d\mu. \quad (2.27)$$

So far we use ε to perform the asymptotic analysis more conveniently. In numerical implementation, one should drop ε in the coupling model (2.23)-(2.26) by setting $\varepsilon = 1$. The domain is diffusive if $Q \approx O(1/\varepsilon)$.

2.3. Properties of the coupling. The reconstruction of the distribution function f_R^ε from the solution of the diffusion equation n_R^ε retains both the zero-th and first order terms of the Hilbert expansion. This is necessary in order to recover the diffusion equation on the entire real line when both regions are diffusive (see below). Eqs. (2.23) and (2.25) can be combined into

$$\varepsilon^2\partial_t f_L^\varepsilon + \varepsilon h\mu\partial_x f_L^\varepsilon - hQ(f_L^\varepsilon) = \varepsilon^2 h\mu\partial_x(Q^{-1}(\mu)\partial_x n_R^\varepsilon), \quad (2.28)$$

showing that the n_R^ε enters the equation for f_L^ε in an order $O(\varepsilon^2)$ term. In the case where $S = \sigma(x)/2$ does not depend on μ, this equation becomes:

$$\varepsilon^2\partial_t f_L^\varepsilon + \varepsilon h\mu\partial_x f_L^\varepsilon - hQ(f_L^\varepsilon) = \varepsilon^2 h\mu^2\partial_x(\sigma^{-1}\partial_x n_R^\varepsilon). \quad (2.29)$$

We now prove that if both regions are diffusive, we recover the global diffusion equation (2.6) for $n = n_L + n_R$.

Proposition 2.5. *As $\varepsilon \to 0$, the solution f_L^ε, n_R^ε of system (2.23)-(2.27) converges to the pair n_L, n_R, the solution of the diffusion system:*

$$\partial_t n_L - h[\partial_x(D(x)\partial_x n_L) + \partial_x(D(x)\partial_x n_R)] = 0, \quad (2.30)$$
$$\partial_t n_R - (1-h)[\partial_x(D(x)\partial_x n_R) + \partial_x(D(x)\partial_x n_L)] = 0, \quad (2.31)$$

with initial data

$$n_L|_{t=0} = hn_0, \quad n_R|_{t=0} = (1-h)n_0, \quad n_0 = \frac{1}{2}\int_{-1}^{1} f_0\, d\mu. \quad (2.32)$$

In particular, $n = n_L + n_R$ is the solution of the diffusion equation (2.6) with initial condition n_0.

Proof: The proof is similar to that of proposition 2.4. The term involving n_R^ε in the transport equation for f_L^ε is of order $O(\varepsilon^2)$. Therefore, it does not induce any change in the expression of the first two equations of the Hilbert expansion (2.9) and (2.10). Eq. (2.11) is modified into:

$$hQ(f_L^{(2)}) = h\mu\partial_x f_L^{(1)} + \partial_t f_L^{(0)} + h\mu\partial_x(Q^{-1}(\mu)\partial_x n_R). \quad (2.33)$$

Integrating it with respect to μ in order to express the solvability condition for $f_L^{(2)}$, we obtain:

$$\partial_t n_L^\varepsilon + h\partial_x j_L^\varepsilon = -h\partial_x((\frac{1}{2}\int Q^{-1}(\mu)\mu\, d\mu)\partial_x n_R)\,,$$

thus leading to (2.30). We use the expression of j_L from (2.15), (2.13), giving $j_L = -D\partial_x n_L$. Inserting this expression into (2.24) yields (2.31), which concludes the proof. ∎

Therefore, our coupled kinetic-diffusion model is consistent with the diffusion equation on the entire real line when the kinetic region $(-\infty, a)$ is also in the diffusive regime.

An important issue is positivity. Indeed, a distribution function being a density in phase-space is a positive quantity. Therefore, we should ensure that $f_L^\varepsilon + f_R^\varepsilon$, which is our approximation of f, remains positive or at least, close to positive. Since the signs of the coupling terms in eqs. (2.23)-(2.24) are not determined, both f_L^ε and n_R^ε could become negative.

In fact, outside the buffer zone, i.e. in the intervals $(-\infty, a]$ or $(b, +\infty]$, the coupling terms vanish identically, and we solve either a standard transport equation or a standard diffusion equation. Therefore, loss of positivity can only originate from the buffer zone $[a, b]$. This region is a diffusive region for both f_L^ε and f_R^ε, since the conditions which ensure that the diffusion approximation is valid for f_R^ε (i.e. $Q = O(1)$) also make the diffusion approximation valid for f_L^ε. In this case, both f_L^ε and f_R^ε are close (at order ε) to the solutions n_R and n_L of the diffusion equations (2.30), (2.31). But since $n_R + n_L$ solves the classical diffusion equation, it remains positive. Therefore, in the buffer zone, $f_L^\varepsilon + f_R^\varepsilon$ are close, up to order $0(\varepsilon)$ terms, to a positive function.

Consequently, if losses of positivity occur in the buffer zone, they will remain small of order ε. If they are ultimately propagated outside the buffer zone, they will remain small of this order everywhere. Therefore, although we cannot prove that our method preserves positivity, we have solid indications that negative values, if they occur, will remain small. Our numerical simulations did not exhibit any loss of positivity so far (see next section).

REMARK 2.1. *There is an alternate coupling strategy to (2.23)-(2.27). It consists in the following system:*

$$\varepsilon^2\partial_t f_L^\varepsilon + \varepsilon h\mu\partial_x f_L^\varepsilon + \varepsilon h\mu\partial_x n_R^\varepsilon = Q(f_L^\varepsilon)\,, \tag{2.34}$$

$$\partial_t n_R^\varepsilon - \partial_x((1-h)D(x)\partial_x n_R^\varepsilon) - \partial_x((1-h)D(x)\partial_x n_L^\varepsilon) + (1-h)\partial_x j_L^\varepsilon = 0\,, \tag{2.35}$$

$$n_L^\varepsilon = \frac{1}{2}\int_{-1}^{1} f_L^\varepsilon\, d\mu\,, \quad j_L^\varepsilon = \frac{1}{2\varepsilon}\int_{-1}^{1} f_L^\varepsilon \mu\, d\mu\,. \tag{2.36}$$

This model is more heuristic since it is not obtained from a diffusion approximation of the coupled kinetic equations (2.16), (2.17). However, it shares with (2.23)-(2.27) the property of relaxing towards the solution of the diffusion equation on the whole real line when both regions are diffusive (we leave the details of the proof to the reader).

3. Numerical Method. In this section we introduce a new (spatially discrete) numerical method for the coupling problem. In fact, this numerical scheme can be used for a discretization of the transport equation with different order of magnitude in ϵ, in the spirit of *asymptotic-preserving method* [17, 20, 21, 22, 23, 24, 26, 30, 31, 32] that works uniformly with respect to the mean free path. However, this new asymptotic preserving spatial discretization method has not been reported in the literature.

3.1. Parity formulation. We explain the new scheme using the transport equation with isotropic scattering (2.4). It is based on the parity form of the transport equation. This is a standard form used to construct asymptotic preserving scheme [1, 24, 36]. For anisotropic scattering, if $S(x, \mu, \mu')$ is even in both μ and μ', one can also use the parity form. For isotropic scattering (2.4), the coupling problem (2.23)-(2.26) becomes

$$\begin{aligned}\varepsilon^2 \partial_t f_L + \varepsilon h \mu \partial_x f_L + \varepsilon h \mu \partial_x f_R & \\ = h\sigma \left[\frac{1}{2} \int_{-1}^{1} (f_L(\mu') + f_R(\mu')) d\mu' - f_L(\mu) - f_R(\mu) \right] , & \qquad (3.1)\end{aligned}$$

$$\partial_t n_R - \frac{1}{3}(1-h)\partial_x(\sigma(x)^{-1}\partial_x n_R) + (1-h)\partial_x j_L = 0 \,, \qquad (3.2)$$

$$f_R = n_R - \varepsilon \frac{\mu}{\sigma} \partial_x n_R \,, \qquad (3.3)$$

$$j_L^\varepsilon = \frac{1}{\varepsilon} \int_0^1 f_L \mu \, d\mu \,. \qquad (3.4)$$

Applying (3.3) in (3.1) one gets

$$\varepsilon^2 \partial_t f_L + \varepsilon h \mu \partial_x f_L - \varepsilon^2 h \mu^2 \partial_x (\sigma^{-1} \partial_x n_R) = h\sigma \left[\frac{1}{2} \int_{-1}^{1} f_L(\mu') d\mu' - f_L(\mu) \right] , \qquad (3.5)$$

$$\partial_t n_R - \frac{1}{3}(1-h)\partial_x(\sigma(x)^{-1}\partial_x n_R) + (1-h)\partial_x j_L = 0 \,, \qquad (3.6)$$

$$j_L = \frac{1}{\varepsilon} \int_0^1 f_L \mu \, d\mu \,. \qquad (3.7)$$

Define the even- and odd-parities, for $\mu > 0$, as

$$f^E(t,x,\mu) = \frac{1}{2}\,[f(t,x,\mu) + f(t,x,-\mu)], \qquad (3.8)$$

$$f^O(t,x,\mu) = \frac{1}{2\epsilon}\,[f(t,x,\mu) - f(t,x,-\mu)]. \qquad (3.9)$$

Then

$$n(t,x) = \frac{1}{2} \int_{-1}^{1} f(t,x,\mu)\, d\mu = \int_0^1 f^E(t,x,\mu)\, d\mu \,, \qquad (3.10)$$

$$j(t,x) = \frac{1}{2\epsilon} \int_{-1}^{1} f(t,x,\mu)\mu\, d\mu = \int_0^1 f^O(t,x,\mu)\mu\, d\mu \,. \qquad (3.11)$$

With the parities, from now on we only consider $\mu > 0$. First, we split (3.1) and (3.2) as two equations, one for μ and one for $-\mu$ (from now no we omit the superscript):

$$\varepsilon^2\partial_t f_L(\mu)+\varepsilon h\mu\partial_x f_L(\mu)-\varepsilon^2 h\mu^2\partial_x(\sigma^{-1}\partial_x n_R)$$
$$=h\sigma\left[\frac{1}{2}\int_{-1}^{1} f_L(\mu')d\mu'-f_L(\mu)\right],\quad \text{for}\quad x<b\,, \tag{3.12}$$
$$\varepsilon^2\partial_t f_L(\mu)+\varepsilon h\mu\partial_x f_L(-\mu)-\varepsilon^2 h\mu^2\partial_x(\sigma^{-1}\partial_x n_R)$$
$$=h\sigma\left[\frac{1}{2}\int_{-1}^{1} f_L(\mu')d\mu-f_L(-\mu)\right],\quad \text{for}\quad x<b\,, \tag{3.13}$$
$$\partial_t n_R-\frac{1}{3}(1-h)\partial_x(\sigma(x)^{-1}\partial_x n_R^{\varepsilon})+(1-h)\partial_x j_L^{\varepsilon}=0\,,\quad \text{for}\quad x>a\,, \tag{3.14}$$
$$j_L=\frac{1}{\varepsilon}\int_0^1 f_L^O\mu\,d\mu\,. \tag{3.15}$$

Adding and subtracting the two equations in (3.12) and (3.13) lead to

$$\epsilon^2\partial_t f_L^E+\epsilon h\mu\partial_x f_L^O-\varepsilon^2 h\mu^2\partial_x(\sigma^{-1}\partial_x n_R)=h\sigma\left(\int_0^1 f_L^E\,d\mu-f_L^E\right), \tag{3.16}$$
$$\epsilon^2\partial_t f_L^O+\epsilon h\mu\partial_x f_L^E=-h\sigma f_L^O,\quad \text{for}\quad x<b\,, \tag{3.17}$$

Our system now consists of eqns (3.16), (3.17), (3.14) and (3.15).

3.2. Asymptotic-preserving spatial discretization using staggered grids. For spatial discretization, let x_j be the mesh point for $i=0,1,\cdots,J$. The even parity will be defined on these mesh points, namely, $f_i^E=f^E(x_i), n_{R,i}=n_R(x_i)$. For the odd-parity we define them on a staggered mesh point $x_{i+1/2}=(x_i+x_{i+1})/2$: $f_{i+1/2}^O=f^O(x_{i+1/2})$. This definition guarantees that when $\epsilon\to 0$ one ends up at a three point rather than five point scheme for the diffusion equation. This is crucial for the coupling problem (especially when the coupling is via a sharp interface). Previous AP schemes [23, 24, 26] for diffusive transport equations yield five point stencils in this limit.

Let $\sigma_i=\sigma(x_i), \sigma_{i+1/2}=\frac{1}{2}(\sigma_i+\sigma_{i+1}), h_i=h(x_i), h_{i+1/2}=h(x_{i+1/2})$. The spatially discrete scheme for the coupling problem (3.16), (3.17), (3.14), (3.15) is given by center difference on a staggered grid:

$$\epsilon^2\partial_t f_{L,i}^E+\epsilon h_i\mu\frac{f_{L,i+1/2}^O-f_{L,i-1/2}^O}{\Delta x}$$
$$-\epsilon h_i\mu^2\frac{1}{(\Delta x)^2}\left[\sigma_{i+1/2}^{-1}(n_{R,i+1}-n_{R,i})-\sigma_{i-1/2}^{-1}(n_{R,i}-n_{R,i-1})\right]$$
$$=h_i\sigma_i\left[\int_0^1 f_{L,i}^E\,d\mu-f_{L,i}^E\right], \tag{3.18}$$
$$\epsilon^2\partial_t f_{L,i+1/2}^O+\epsilon h_{i+1/2}\,\mu\frac{f_{L,i+1}^E-f_{L,i}^E}{\Delta x}=-h_{i+1/2}\sigma_{i+1/2}f_{L,i+1/2}^O, \tag{3.19}$$
$$\partial_t n_{R,i}-(1-h_i)\frac{1}{(\Delta x)^2}\left[\sigma_{i+1/2}^{-1}(n_{R,i+1}-n_{R,i})-\sigma_{i-1/2}^{-1}(n_{R,i}-n_{R,i-1})\right]$$
$$+(1-h_i)\frac{j_{L,i+1/2}-j_{L,i-1/2}}{\Delta x}=0\,, \tag{3.20}$$
$$j_{L,i+1/2}=\frac{1}{\varepsilon}\int_0^1 f_{L,i+1/2}^O\mu\,d\mu\,. \tag{3.21}$$

This is a second order approximation. To verify that it is asymptotic-preserving, for $\epsilon << 1$, the leading order approximation of (3.18) gives

$$f^E_{L,i} = \int_0^1 f^E_{L.i}\, d\mu \equiv n_{L,i} \tag{3.22}$$

while (3.19) gives

$$f^O_{L,i+1/2} = -\epsilon \frac{\mu}{\sigma_{i+1/2}} \frac{f^E_{L,i+1} - f^E_{L,i}}{\Delta x} \,. \tag{3.23}$$

Applying (3.22) and (3.23) into (3.18) and integrating over μ, we get

$$\begin{aligned} \partial_t \rho^E_{L,i} - h_i \frac{1}{3(\Delta x)^2} \left[\sigma^{-1}_{i+1/2}(n_{L,i+1} - n_{L,i}) - \sigma^{-1}_{i-1/2}(n_{L,i} - n_{L,i-1}) \right] & \\ -h_i \frac{1}{3(\Delta x)^2} \left[\sigma^{-1}_{i+1/2}(n_{R,i+1} - n_{R,i}) - \sigma^{-1}_{i-1/2}(n_{R,i} - n_{R,i-1}) \right] = 0 \,, & \end{aligned} \tag{3.24}$$

which is a three point second order approximation to (2.20) with $D = \sigma^{-1}$.

Since the space discretization is a centered-difference one, in order to ensure stability of the time discretization, one can use a so-called *I-stable* ODE solver. An I-stable solver is a scheme for ODEs whose stability region contains part of the imaginary axis. The third and fourth order explicit Runge-Kutta methods are I-stable, among other schemes. An I-stable ODE solver is particularly well suited for convection problems where the convection term is discretized using centered differences, since the spectrum of a centered difference operator is purely imaginary and an I-stable scheme, unlike the forward Euler method, will be stable with a suitable choice of the time step [4, 16, 38]. We would like to remark that for steady state computations, the convergence to the steady state for such an explicit solver is very slow, and some acceleration techniques, such as the diffusion synthetic acceleration [2], can be used but will not be explored in this article.

For discretization in the velocity space, we use the standard discrete-ordinate method with Gaussian quadrature over $(0, 1)$ [35].

4. Numerical Examples. In this section we present several numerical examples on the coupling model (3.1)-(3.4) by the numerical schemes described in the previous section. We solve the problem in domain $[0, 1]$ with Dirichlet boundary condition

$$f(t, 0, \mu) = f_l(\mu) \,, \qquad f(t, 1, -\mu) = f_r(-\mu) \,, \qquad \mu > 0 \,.$$

In these examples $\epsilon = 1$, and the value of σ characterizes the nature of the regime (transport or diffusive). We use 1001 points to solve the transport equation in the entire domain as the "exact" solution, and 25 points for the numerical approximations. We use three choices of h that are piecewise linear: 1 for $x \le a$, 0 at $x > b$, and a line connecting 1 at a and 0 at b with $a = 0.2912, b = 0.7072$; $a = 0.416, b = 0.5824$; and $a = b = 0.5$ respectively. The last set gives a step function. The buffer zone is always chosen to be symmetric and centered at $x = 0.5$. The "exact" solution is given by the solid line, while the numerical results are given by "o", "x" and "*" for the three different sets of a and b respectively. We compare both transient and steady state solutions.

Example 1. We first test the case when both side of the domain are diffusive in the entire domain, namely, $\sigma(x) >> 1$. We take $\sigma(x) \equiv 100$, $f_l(\mu) = 3, f_r(\mu) = 0$ and the initial condition

$$f(0, x, \mu) = 3x^2 .$$

The solution to the diffusion equation (2.20) with $D = \sigma^{-1}$ should be a line connecting 3 to 0. The numerical results at $t = 1$ and at steady state are plotted in Fig. 4.1. One can see that the numerical results match the "exact" solution quite well, while the choice of h seems to have little influence on the numerical solution.

Example 2. We take $\sigma(x) = 2$ for $x < 0.45$, $\sigma(x) = 100$ for $x > 0.55$. $\sigma(x)$ is a linear function interpolating 2 and 100 for $0.45 \leq x \leq 0.55$. The boundary and initial conditions are the same as in Example 1. Thus the domain $[0, 0.45]$ is in the kinetic regime, while the domain $[0.55, 1]$ is diffusive. The results at $t = 0.5$ and at steady state for $n = n_L + n_R$ are depicted in Fig. 4.2(a) for several different choices of a and b. As one can see, for the steady state solution, the choice of h has little influence on the numerical results which match well with the "exact" solution. For the transient solution, the first set of parameters for the buffer zone (which is much larger than the domain for nonconstant σ) yields poor approximation in both the buffer zone and the transport domain, while in the diffusion domain the accuracy is as good as the other two buffer zones. This experiment indicates that the buffer zone should be within the transition region of σ.

In order to compare the effect of regularity of h on the numerical solution, we compare the piecewise linear h corresponding to $a = 0.2912, b = 0.7072$ ('x' in top of Fig.4.3) and $h = 0.5(1 - \tanh(30(x - 0.5))) \in C^\infty$ ('o' in top of Fig.4.3). The numerical results at $t = 0.5$ are given in the bottom of Fig.4.3. The numerical results are comparable.

For the same C^∞-function h, we compare the effect of mesh refinement on the numerical solution. In Fig.4.4 we compare the numerical results obtained by 25 and 50 points respectively. The discrete h looks more regular in the finer mesh. The numerical results look similar, indicating that the regularity of h plays insignificant role in the coupling algorithm.

Example 3. This problem is the same as Example 2 except the boundary condition at $x = 0$, where we take an anisotropic one $f_l(\mu) = 3\mu + 1$ at $x = 0$. The numerical results at the steady state for the three piecewise linear h corresponding to the three different sizes of the buffer zone are given in Fig.4.5, which match quite well with the "exact" solution.

5. Conclusion. In this paper, we have presented a model which allows to handle the transition between a kinetic and a diffusive region in a smooth way. In the transition region both models are solved and the solution of the original transport equation is recovered by adding up the solutions of each model. The advantage of this coupling is that no boundary condition nor any iteration process at the overlapping zone is needed, as is for a typical domain decomposition method. The numerical discretization in the kinetic region is based on the parity formulation of the transport equation and the use of a new asymptotic-preserving scheme. Numerical experiments show that the coupling model describes quantitatively the behavior of the original transport equation, for both transient and steady state solutions, if the buffer zone is chosen inside the transition zone.

Further development of this work will include robust time discretization, multidimensional problems and the extensions to more complex kinetic models such as

Drift-Diffusion or Energy-Transport models in semiconductors or the Boltzmann-BGK model of rarefied gas dynamics.

REFERENCES

[1] M.L. Adams, *Even-Parity Finite-Element Transport Methods in the Diffusion Limit*, Progress in Nuclear Energy, 25 (1991), pp. 159-198.

[2] R.E. Alcouffe, *Diffusion synthetic acceleration methods for the diamond-difference discrete-ordinate equations*, Nucl. Sci. Eng., 64 (1977), pp. 344-355.

[3] G. Bal, and Y. Maday, *Coupling of Transport and Diffusion Models in Linear Transport Theory*, Math. Modeling and Numer. Anal., 36 (2002), pp. 69–86.

[4] W. Bao, and S. Jin, *High order I-stable centered difference schemes for viscous compressible flows*, J. Comp. Math. 21 (2003), pp. 101-112.

[5] C. Bardos, R. Santos, and R. Sentis, *Diffusion approximation and computation of the critical size*, Trans. A. M. S., 284 (1984), pp. 617–649.

[6] A. Bensoussan, J.-L. Lions, and G.C. Papanicolaou, *Boundary layers and homogenization of transport processes*, Publ. Res. Inst. Math. Sci., 15 (1979), pp. 53–157.

[7] J.-F. Bourgat, P. Le Tallec, B. Perthame, and Y. Qiu, *Coupling Boltzmann and Euler equations without overlapping*, in Domain decomposition methods in science and engineering (Como, 1992), 377–398, Contemp. Math. **157**, Amer. Math. Soc., Providence, RI, 1994.

[8] S. Brunner, E. Valeo, and J. P. Krommes, *Linear delta-f simulation of non-local electron heat transport*, Physics of plasmas, 7 (2000), pp. 2810–2823.

[9] C. Buet, S. Cordier, B. Lucquin-Desreux, and S. Mancini, *Diffusion limit of the Lorentz model: asymptotic preserving schemes*, to appear in Math. Modeling and Numer. Anal..

[10] S. Chandrasekhar, Radiative Transfer, Dover, 1960.

[11] N. Crouseilles, *Dérivation de modèles couplés dérive-diffusion/cinétique par une méthode de décomposition en vitesse*, C. R. Acad. Sci. Paris, Ser. I, 334 (2002), pp. 827-832.

[12] N. Crouseilles, P. Degond, and M. Lemou, *Hybrid kinetic/fluid models for nonequilibrium systems*, C. R. Acad. Sci. Paris. Ser. I, 336 (2003), pp 359 - 364.

[13] N. Crouseilles, P. Degond, and M. Lemou, *A hybrid kinetic-fluid model for solving the gas dynamics Boltzmann-BGK equation*, manuscript, submitted.

[14] P. Degond, and C. Schmeiser, *Kinetic boundary layers and fluid-kinetic coupling in semiconductors*, Transport Theory Statist. Phys., **28** (1999), pp. 31–55.

[15] S. Dellacherie, *Kinetic fluid coupling in the field of the atomic vapor laser isotopic separation: numerical results in the case of a mono-species perfect gas*, presented at the 23rd International Symposium on Rarefied Gas Dynamics, Whistler (British Columbia), July 2002.

[16] W. E, and J.-G. Liu, *Vorticity boundary condition and related issues for finite difference schemes,* J. Comput. Phys., 124 (1996), pp. 368-382.

[17] F. Golse, S. Jin, and C.D. Levermore, *The Convergence of Numerical Transfer Schemes in Diffusive Regimes, I. The Dicrete-Ordinate Method*, SIAM J. Num. Anal., 36 (1999), pp. 1333–1369.

[18] F. Golse, S. Jin, and C.D. Levermore, *A Domain Decomposition Analysis for a Two-Scale Linear Transport Problem*, Math. Model Num. Anal., to appear.

[19] M. Günther, P. Le Tallec, J.-P. Perlat, and J. Struckmeier, *Numerical modeling of gas flows in the transition between rarefied and continuum regimes. Numerical flow simulation I*, (Marseille, 1997), 222–241, Notes Numer. Fluid Mech., 66, Vieweg, Braunschweig, 1998.

[20] S. Jin, *Efficient Asymptotic-Preserving (AP) Schemes for Some Multiscale Kinetic Equations*, SIAM J. Sci. Comp., 21 (1999), pp. 441-454.

[21] S. Jin, and C.D. Levermore, *The Discrete-Ordinate Method in Diffusive Regimes*, Transp. Theory Stat. Phys., 20 (1991), pp. 413–439.

[22] S. Jin, and C.D. Levermore, *Fully Discrete Numerical Transfer in Diffusive Regimes*, Transp. Theory Stat. Phys., 22 (1993), pp. 739-791.

[23] S. Jin, L. Pareschi, and G. Toscani, *Diffusive Relaxation Schemes for Multiscale Discrete-Velocity Kinetic Equations*, SIAM J. Num. Anal., 35 (1998), pp. 2405-2439.

[24] S. Jin, L. Pareschi, and G. Toscani, *Uniformly Accurate Diffusive Relaxation Schemes for Multiscale Transport Equations*, SIAM J. Num. Anal., 38 (2000), pp. 913-936.

[25] A. Klar, *Convergence of alternating domain decomposition schemes for kinetic and aerodynamic equations*, Math. Methods Appl. Sci., 18 (1995), pp. 649–670.

[26] A. Klar, *Asymptotic-induced domain decomposition methods for kinetic and drift-diffusion semiconductor equations*, SIAM J. Sci. Comput., 19 (1998), pp. 2032–2050.

[27] A. Klar, *An Asymptotic-Induced Scheme for Nonstationary Transport Equations in the Diffusive Limit*, SIAM J. Num. Anal., 35 (1998), pp. 1073-1094.

[28] A. Klar, H. Neunzert, and J. Struckmeier, *Transition From Kinetic Theory to Macroscopic Fluid Equations: a Problem for Domain Decomposition and a Source for New Algorithm*, Transp. Theory and Stat. Phys., 29 (2000), pp. 93–106.

[29] A. Klar, and N. Siedow, *Boundary layers and domain decomposition for radiative heat transfer and diffusion equations: applications to glass manufacturing process*, European J. Appl. Math., 9 (1998), pp. 351–372.

[30] E.W. Larsen, *The Asymptotic Diffusion Limit of Discretized Transport Problems*, Nucl. Sci. Eng., 112 (1992), pp. 336-346.

[31] E.W. Larsen, and J.E. Morel, *Asymptotic Solutions of Numerical Transport Problems in Optically Thick, Diffusive Regimes II*, J. Comput. Phys., 83 (1989), pp. 212–236.

[32] E.W. Larsen, J.E. Morel, and W.F. Miller Jr., *Asymptotic Solutions of Numerical Transport Problems in Optically Thick, Diffusive Regimes*, J. Comput. Phys., 69 (1987), pp. 283–324.

[33] P. Le Tallec, and F. Mallinger, *Coupling Boltzmann and Navier-Stokes equations by half fluxes*, J. Comput. Phys., 136 (1997), pp. 51–67.

[34] P. Le Tallec, and M. Tidriri, *Convergence analysis of domain decomposition algorithms with full overlapping for the advection-diffusion problems*, Math. Comp., 68 (1999), pp. 585–606.

[35] E.E. Lewis, and W.F. Miller Jr., *Computational Methods of Neutron Transport*, Wiley-Interscience, New York (1984).

[36] W.F. Miller Jr., *An Analysis of the Finite-Differenced, Even-Parity Discrete-Ordinate Equations in Slab Geometry*, Nucl. Sci. Eng., 108 (1990), pp. 247–266.

[37] M. Tidriri, *New Models for the Solution of Intermediate Regimes in Transport Theory and Radiative Transfer: Existence Theory, Positivity, Asymptotic Analysis, and Approximations*, J. Stat. Phys., 104 (2001), pp. 291-325.

[38] R. Vichnevtsky, *Stability charts in the numerical approximation of partial differential equations: a review*, Math. Comput. Simulation, XXI (1979), pp. 170-177.

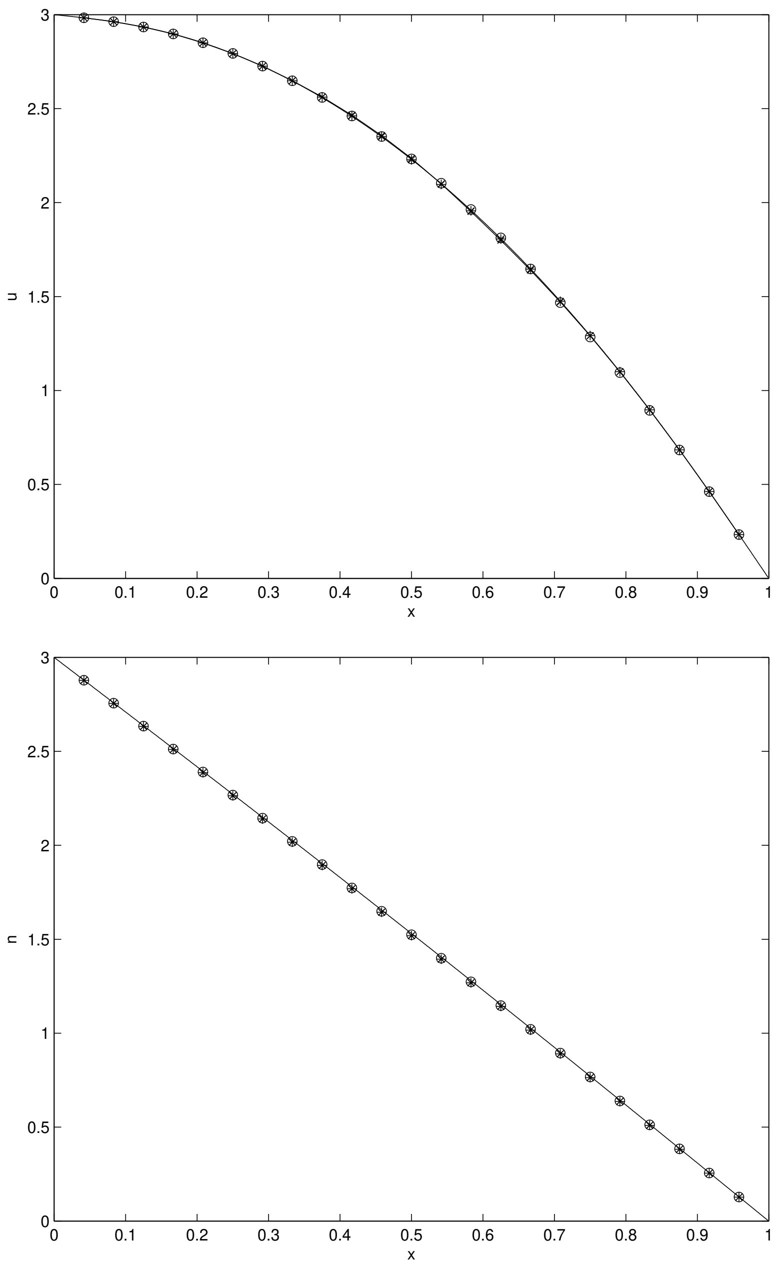

FIG. 4.1. *The numerical solution of* n *for Example 1 at* $t = 1$ *(top) and at steady state (bottom) of Example 1. The solid line is the solution of the transport equation in the entire domain computed using* 1001 *points, while the other three symbols represent numerical solution of the coupling model with* 25 *grid points and three different sizes of the buffer zone.*

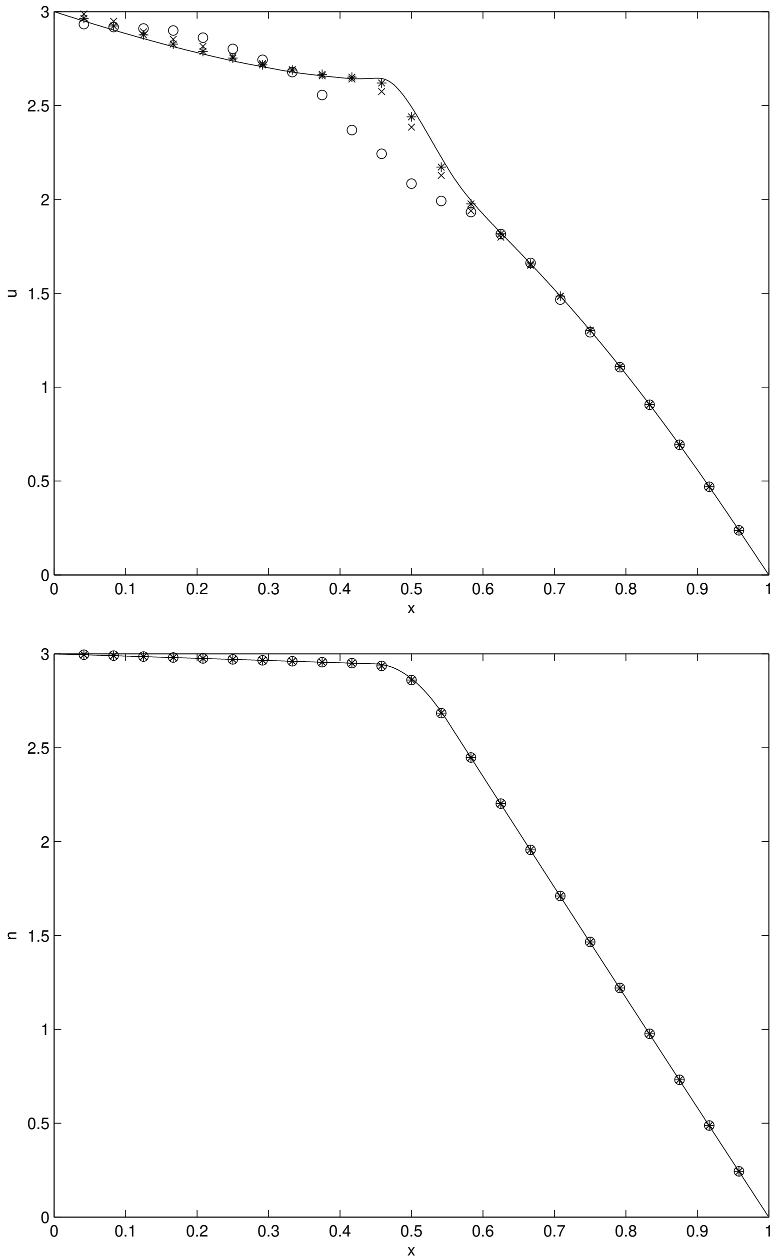

FIG. 4.2. *The numerical solution of* n *for Example 2 at* $t = 0.5$ *(top) and at steady state (bottom) of Example 2. The Solid line is the solution of the transport equation in the entire domain computed using* 1001 *points, while the other three symbols represent numerical solutions of the coupling model with* 25 *grid points and three different sizes of the buffer zone.*

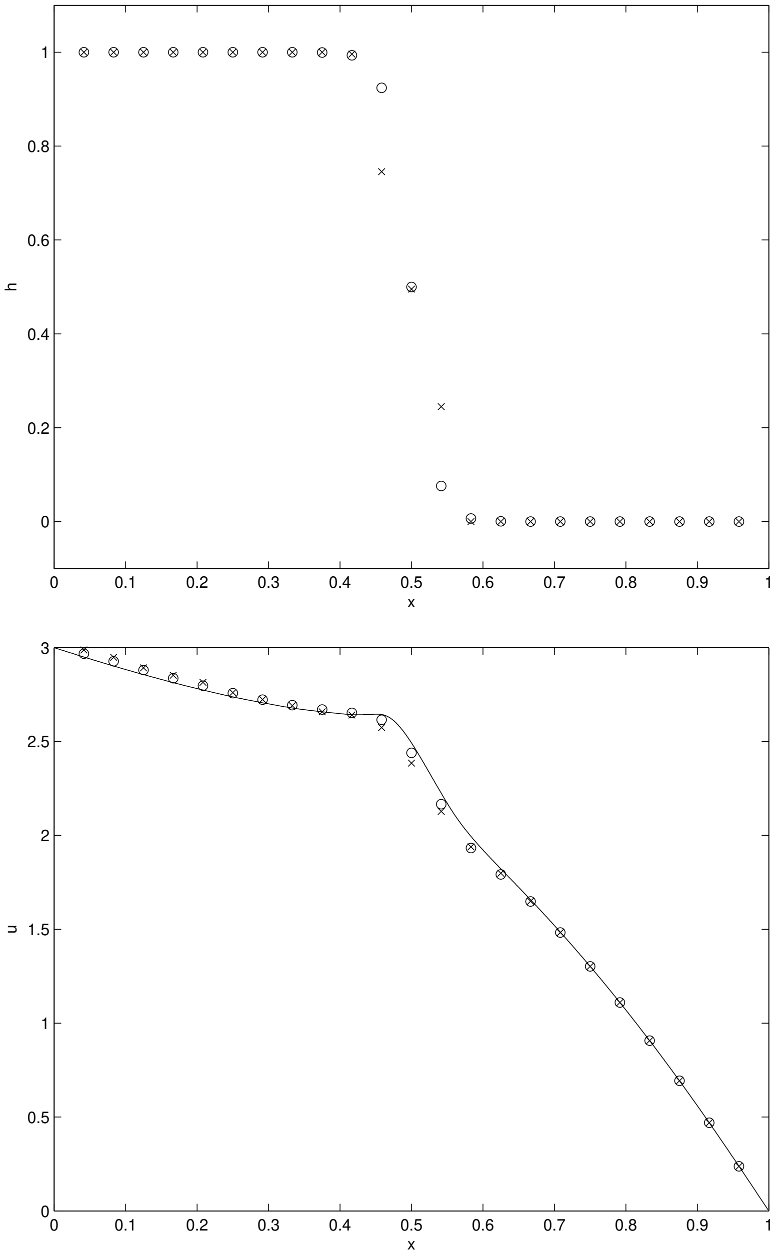

FIG. 4.3. *Example 2. Top: Comparison of different h: piecewise linear "x", C^∞ "o". Bottom: The corresponding numerical results for these h-functions vs. the "exact" solution at $t = 0.5$.*

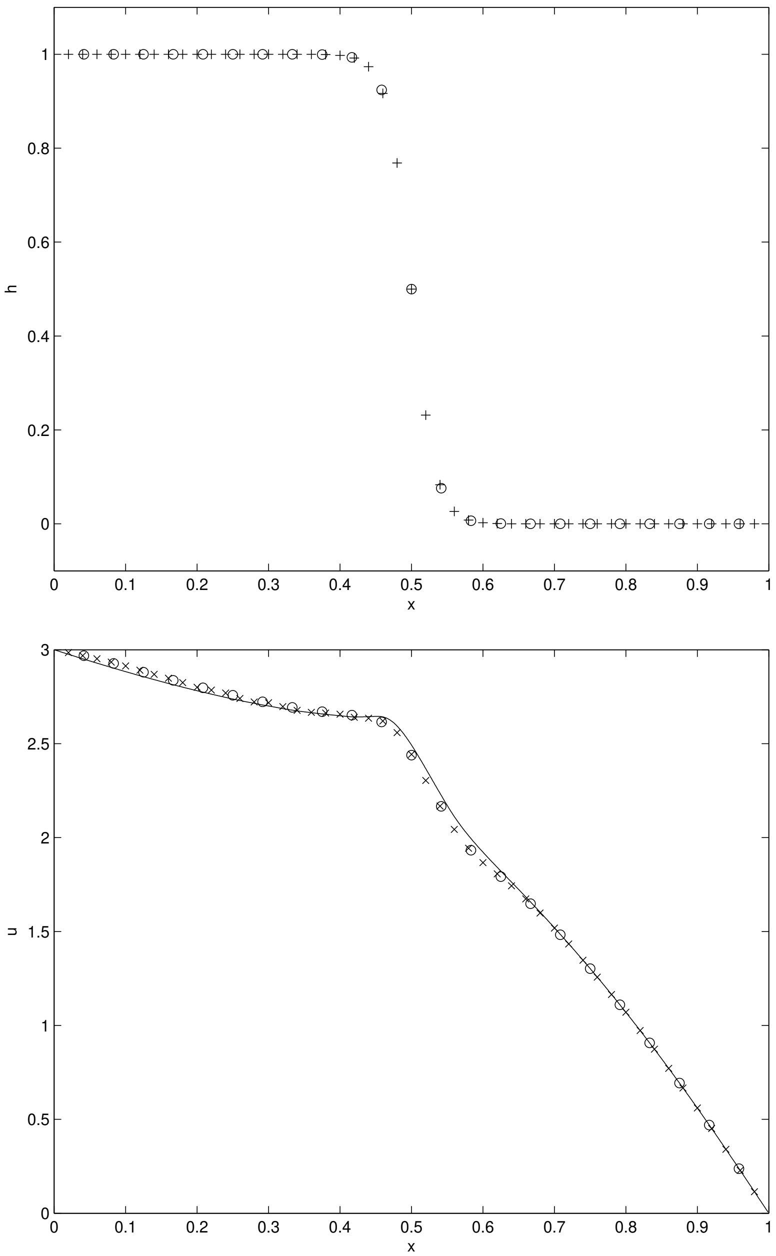

FIG. 4.4. *Example 2. Top: Comparison of same C^∞-function h with different mesh sizes: 25 grid points "o", 50 grid points "x". Bottom: The corresponding numerical results for these h-functions vs. the "exact" solution at* $t = 0.5$.

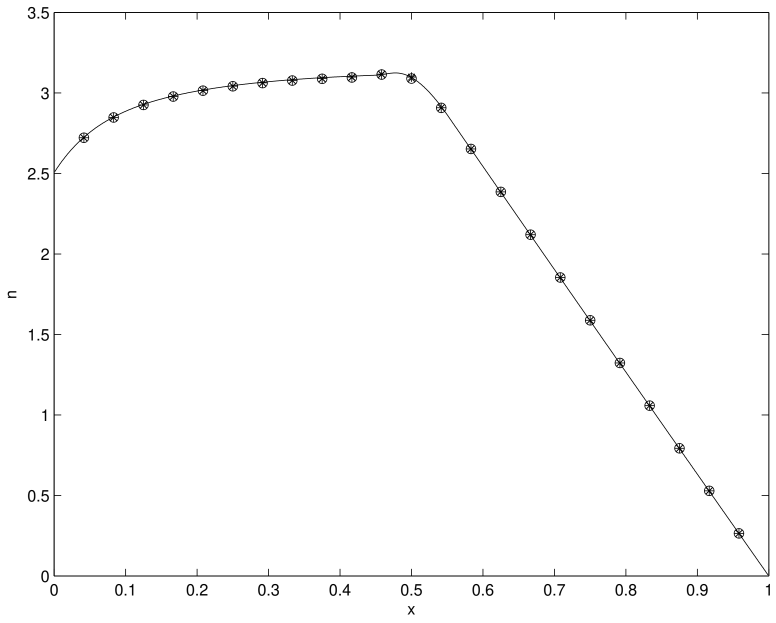

FIG. 4.5. *The numerical steady state solutions* $n = n_L + n_R$ *of Example 3. Solid line is the solution of the transport equation in the entire domain cumputed using* 1001 *points, while the other three symbols represent numerical solution of the coupling model with* 25 *grid points and three different sizes of the buffer zone.*